30th Congress of the International Council of the Aeronautical Sciences
DCC, Daejeon, Korea ; September 25-30, 2016

AEROPROPULSIVE PERFORMANCE ANALYSIS OF THE NOVA CONFIGURATIONS

Ludovic Wiart*, Olivier Atinault*, Jean-Christophe Boniface*, Raphaël Barrier*
***ONERA - The French Aerospace Lab**

Keywords: *Aerodynamics, Propulsion, BLI, Fan, UHBR, Actuator Disk*

Abstract

In order to evaluate the potential of UHBR (Ultra High Bypass Ratio) turbofan engines for the replacement of existing medium-haul aircraft, four different NOVA (Nextgen Onera Versatile Aircraft) aircraft geometries have been defined at ONERA with a particular focus on engine integration options. In this paper, the focus is on the two rear-fuselage engine configurations, consisting of a classically pylon-mounted nacelle and of a buried engine with a BLI (boundary layer ingesting) inlet. These two configurations are a good basis for studying the challenges and benefits of boundary layer ingestion at transonic speed. Although it is assumed that power savings due to BLI have a low dependence on compressibility effects, most studies to date are limited to low Mach number. This is therefore, to the knowledge of the authors, the first published demonstration of an aeropropulsive advantage for a BLI configuration using 3D RANS CFD (Computational Fluid Dynamics) on realistic geometries at high transonic regime (M=0.82). Two different Actuator Disk (AD) formulations have been used to model the fan behavior and a power saving of 5% in favor of the BLI configuration is exhibited in cruise condition.

1 Introduction

The work presented in this paper was performed in the frame of a project funded by the French National Research Agency (ANR) aiming at anticipating the challenges related to UHBR turbofan engines integration on future aircraft. In addition to exploring innovative engine integration options, this on-going project is also focused on numerical and experimental methods for the performance prediction of unconventional designs, such as boundary-layer ingesting engines and unshocked fan nozzle at cruise conditions for instance.

In order to assess the impact of the proposed engine integration options, relevant aircraft geometries had to be selected and designed. It was decided to develop realistic transport aircraft configurations as an alternative to current single-aisle medium-haul aircraft. The considered mission is to carry 180 passengers (with a two-class layout) at a cruise Mach number of 0.82 for a 3000 nautical miles flight. The configurations considered, for a 2025 entry into service, were limited to tube and low wings.

Figure 1 NOVA "BLI" Configuration

Concerning the engine integration study, it was decided to investigate four different possible engine positions. Two configurations were designed as references with rather conventional engine mounts: on pylons under the wing (referred to as the “baseline” configuration) and on the aft fuselage side (referred to as the “podded” configuration). Two innovative configurations were designed, aiming at reducing the mass and drag penalty for the integration of such UHBR turbofan engines. The first one features a modified wing shape, with higher dihedral angle in the inboard portion (similar to a gull wing) in order to accommodate those big engines without having to extend the landing gear legs beyond reasonable limits. It will be referred to as the “gull wing” configuration. The last configuration was designed with a rear semi-buried turbofan fed by a boundary layer ingesting air intake (see Figure 1). This configuration aims at taking advantage of the improved propulsive efficiency inherent to boundary layer ingestion. It will be referred to as the “BLI” (Boundary Layer Ingestion) configuration. The four NOVA configurations are presented in Figure 2.

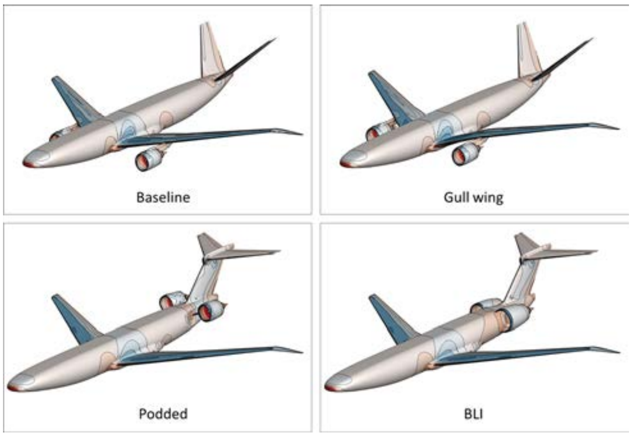

Figure 2 General view of the NOVA configurations

The tools, conceptual studies, preliminary and detailed aerodynamic design work have been the subject of a previous paper [1]. The effect of engine/airframe installation has been investigated on the baseline and gull wing configurations and covered in the same document. In this paper, the focus is on the podded and BLI configurations solely.

The advantages of BLI have been thoroughly described in the literature [2] and can be summarized in the following terms:

- a possible reduction in wetted area due to outer nacelle pylon removal and possibly shorter nacelle. This latter is very dependent on the engine integration on the airframe. In the case of NOVA BLI configuration, this potential gain is in fact cancelled by a longer nacelle, required for correct inlet operation.
- a reduction of jet and wake losses. The idea here is to reenergize the weakened part of the flow over the airframe (the boundary layer) and limit the excess (waste) of energy due to engine jet.

The commonly used metric to quantify those gains is the power-saving coefficient (PSC) which can be expressed as

$$PSC = \frac{P_{Podded} - P_{BLI}}{P_{Podded}} \qquad (1)$$

with P_{Podded} the fan power calculated for the “podded” configuration and P_{BLI} the fan power for the “BLI” configuration calculated at the same net force.

The more boundary layer is ingested, the higher the expected BLI benefit. Here, the idea is to take advantage of a possible BLI benefit for a given UHBR engine and a given wing-body configuration. The potential PSC is therefore highly dependent on the amount of fuselage boundary layer ingested by the engines (about 40 % at cruise). A rapid estimate of the expected PSC for NOVA leads to a 4-5% range as illustrated in Figure 3.

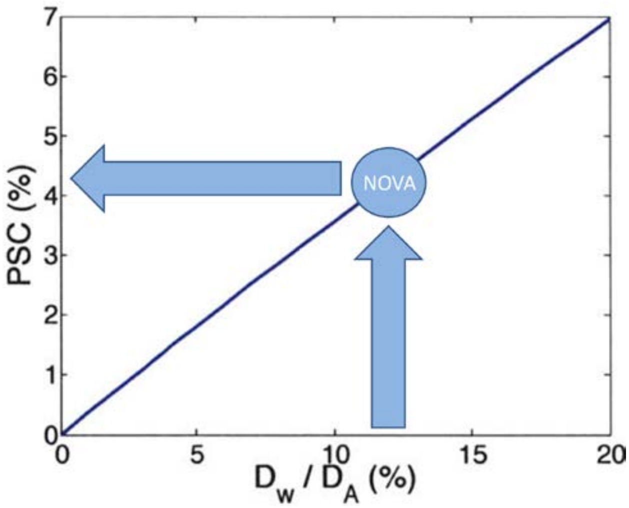

Figure 3 NOVA potential PSC versus percentage of aircraft drag ingested by the engines, original chart from [3], p.50

In order to carry out a more in depth analysis of the potential power saving for a BLI configuration, one has to define a reference non-

BLI configuration to be compared to at the same net force. As described in the literature [4], different choices are available in terms of engine geometry commonality between these two configurations. The choice was made to keep the fan diameter and the nozzle exhaust area constant between the podded and the BLI configurations.

Of course BLI has many implications at system level that should be taken into account before being able to derive the associated fuel burn reduction. For instance, moving the engines closer to the fuselage centerline may reduce the required vertical tail area, the pylon removal should provide some weight saving, leading to a more favorable wing area/thrust couple, and so on. Some regulatory constraints should also be considered, such as the impact of a turbine disk failure on the other engine(s) or the pressurized cabin, or the integration of thrust reversers. Not to mention the capability of a fan to cope with unsteady blade deformation while maintaining an acceptable efficiency.

In this paper, only the aeropropulsive benefit due to BLI is investigated. The emphasis is placed on the fan modeling, two different Actuator Disk (AD) approaches being compared. Tentative PSC figures are obtained from 3D RANS calculations performed on the NOVA podded and BLI configurations.

2 Characteristics of the NOVA fan

As explained earlier, the NOVA configurations were designed in the frame of a broader project, focused on UHBR engine integration. For the needs of this project, a dedicated fan was designed at ONERA. It has 18 blades and delivers a fan pressure ratio (FPR) of 1.4 at design point, with a corrected specific mass flow at rotor plane of 209 kg/s/m². An overview of its geometric characteristics is given in Figure 4, along with its associated Outlet Guide Vane (OGV).

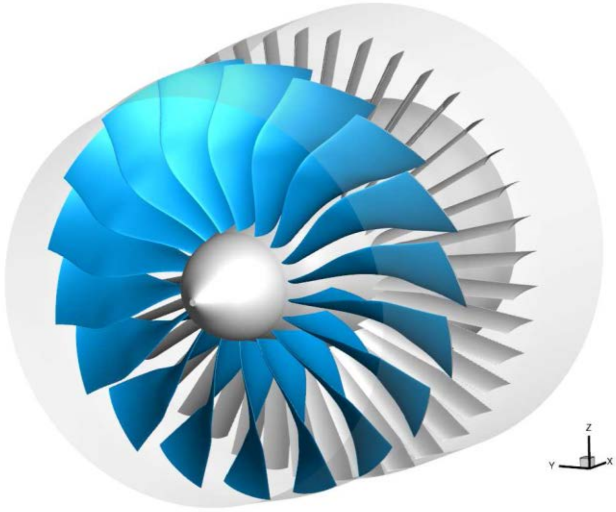

Figure 4 Overview of the NOVA fan

It was designed through steady mixing plane calculations, using the elsA software [5]. The CFD results obtained for different operating points constitute a valuable database. However, that kind of approach is not suited to the case of boundary-layer ingestion, since it is perceived as an unsteady solicitation by the fan. Full annulus URANS calculations would be required in that case, which, coupled with the rest of the aircraft, would lead to pretty heavy calculations. Hence the need for a simplified fan model, compatible with steady computations.

The fan model used for CFD should therefore answer to two different requirements:

- to be able to reproduce the physical action of a fan (and OGV) on the incoming flow to provide reliable PSC data;
- to be as close as possible to the 3D fan in terms of stagnation pressure and temperature jumps, mass flow rate, traction and power.

Good candidates are the Actuator Disk and body-force formulations. However, at the time of this study, only the AD was available in the elsA software.

3 Fan modeling in the *elsA* CFD software

Two Actuator Disk models described next were developed in the elsA software. This was motivated by steady computations for propellers and helicopter rotors operating in freestream conditions. For both models, the surrounding flowfield is computed by CFD and the AD is represented in the structured mesh as a surface of discontinuity without thickness (unlike a body-force model). The mesh topology must be defined accordingly, with upstream and downstream surrounding meshes ensuring a conformal match where the AD surface is introduced as illustrated in Figure 5.

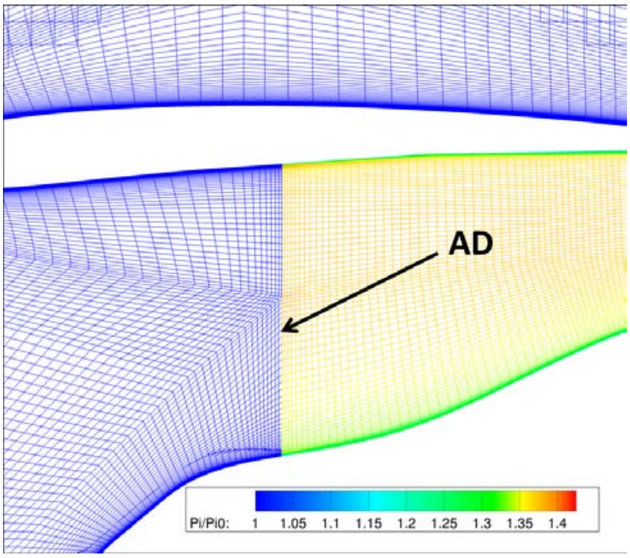

Figure 5 Mesh topology and stagnation pressure jump caused by an AD in a nacelle

Both models were designed to achieve a balance between either prescribed jumps or external forces supplied to the flow and the modification of the flowfield governed by mass conservation, balance of axial and tangential momentum equations and energy. In their respective implementation, assuming steady compressible flows, there is no formal limitation in Mach number. For low-Mach number configurations, both models can be used together with a local low-speed preconditioning formulation of the RANS equations [6]. These two AD models were then further assessed for fan modeling.

3.1 "Propeller" Actuator Disk (ADv2)

3.1.1 Description

This implementation was originally designed to handle propeller configurations [7],[8]. The "propeller" formulation of the AD was first developed from subsonic outlet/inlet boundary conditions for the flow solver, based on the characteristic theory. It will be referred to as the ADv2 model.

At the front mesh interfaces (upstream), a subsonic outlet boundary condition locally prescribes the continuity of the mass flow with respect to corresponding rear interfaces (downstream). At the rear mesh interfaces (downstream), a subsonic inlet boundary condition was formulated with prescribed flow discontinuities, depending on the propeller characteristics. The flow discontinuities are expressed in term of jumps in stagnation pressure, associated stagnation temperature and angular flow deviation in the local propeller reference frame. These discontinuities depend on the radial position on the propeller and on the local Mach number at a given location in the front mesh interface. The input data characterizing the respective jumps of stagnation pressure, stagnation temperature and flow deviation depend on the propeller thrust and torque, and have to be obtained previously either from propeller manufacturers data or from simplified models (lifting line methods, Glauert theory).

3.1.2 Limitations

Applying this formulation of the AD to a ducted fan is actually not obvious and proved to be very challenging numerically.

It was expected that large pressure jumps at the periphery of the disk would lead to the separation of the nacelle internal boundary layer. It appeared very quickly from previous studies that the AD model should include tangential flow deviation, and also that the full nacelle geometry should include a realistic hub. The full AD model with tangential deviation was built using an in-house tool based on the Glauert mean flow theory for a propeller, this theory being an extension of the mono-dimensional Froude theory. The AD could be successfully used with a full model obtained from the Glauert theory applied to a fan geometry operating in low-speed conditions, after this model has been modified to increase the pressure jump and the flow deviation near the hub [9].

However, a lack of numerical robustness was experienced for the NOVA geometries, in some critical flow conditions at cruise speed and high transonic regime, or arising from a prescribed heavy loaded AD, possible inconsistent pressure jumps in the boundary layers, or transient flow solutions. Generally such conditions are responsible for local flow separation in the boundary layer at the hub and casing. This frequently occurs in a design process, within parametric studies, and may cause the divergence of the computational procedure. In many situations, a locally reverse flow was observed across the AD or a non-physical local supersonic flow, in case of strong oscillations in the transient phase of the computations. In such extreme cases, the assumption of uniformly prescribed subsonic outlet at the front side and subsonic inlet at the rear side may be no longer valid. In most cases, a clear violation of the characteristic theory could be noted.

So, it was decided that a more robust numerical implementation had to be considered in the elsA software, accounting for possible subsonic/supersonic inlet/outlet flow conditions occurring on both sides of the AD. Additionally, the reformulation now takes into account that the jump conditions could be applied only selectively according to the local flow pattern, keeping the consistency with the AD modeling outside of the reverse flow areas.

3.2 “Helicopter” Actuator Disk (ADv1)

3.2.1 Description

The “propeller” formulation of the AD described above was also originally used for the simulation of rotorcraft aerodynamics. The main rotor can be viewed as a lifting surface, representing the time-averaged loads in the framework of steady computations of rotor/fuselage interactions. However, in some high-speed forward-flight conditions, as the main lifting rotor is tilted, locally reverse flow conditions were also experienced computationally. This typically arises from suction effects near the leading edge of the AD, with the flow moving through the disk from the pressure to the suction side. Again, inconsistencies with the characteristic theory were responsible for strong oscillations in the numerical procedure.

For helicopter rotor configurations, the issue of local reverse flow was circumvented by drastically reformulating the AD model. This was achieved by modeling the AD with non-uniform external forces and power supplied to the flow, forcing a pressure jump responsible for the rotor global lift and the rotor downwash [10]. In this formulation, which will be referred to as ADv1, there is no need to formulate the AD from inner inflow/outflow boundary conditions, unlike the “Propeller” formulation. A surface source term is simply added to the momentum and energy conservation laws, for the cell interfaces adjacent to the downstream side of the AD. The aerodynamic loads may be computed by an external lifting-line model for the trimmed rotor, to provide the force and power density distribution in the radial and circumferential directions of the AD.

3.2.2 Limitations

Although the “Helicopter” formulation yields a robust numerical procedure and is well adapted to helicopter rotor aerodynamics, or open rotor configurations, severe limitations occurred in its practical implementation to configurations of turbofan engines, reproducing high pressure ratios. As the pressure ratio is increasing, this generates a sharp discontinuity in the flowfield. Strong oscillations were observed in the pressure field in the vicinity of the AD. This behavior is still not yet well understood, and is not reproduced with the “propeller” formulation of the AD.

However, the main weakness of this approach is that the same specified force is applied independently from the incoming flow characteristics (local Mach number, angle…). This is an issue, especially in the case of an aggressive BLI inlet, where strong distortion is expected in the fan plane.

4 Results

4.1 Implementation of the two Actuator Disk approaches on the NOVA configurations

The "helicopter" formulation (ADv1) was tested first, due to its superior numerical robustness. It was used in its most basic form, specifying a single axial force to be applied on the disk surface (a more advanced use would be to provide a force map, based on results from the NOVA fan for instance).

The "propeller" formulation (ADv2) was used after its robustness was improved as described in §3.1.2. The input data was generated using the in-house propeller fast design tool. A blade geometry having characteristics similar to the NOVA fan at design point was generated, and charts were then obtained for different RPM. Although as mentioned in §3.1.2 tangential flow deviation can be necessary to mitigate flow separation downstream of the AD, it is not desirable to have a rotating flow interacting with the fuselage tail, especially for the BLI configuration. Since the OGV is not included in the CFD mesh, it was therefore decided to set the flow deviation jump to zero, the AD acting thus as a complete fan and OGV stage. In order to prevent downstream flow separation, the stagnation pressure jump was made more uniform radially than that of the NOVA fan as illustrated in Figure 6. This also impacts the associated distribution of stagnation temperature jump as a consequence.

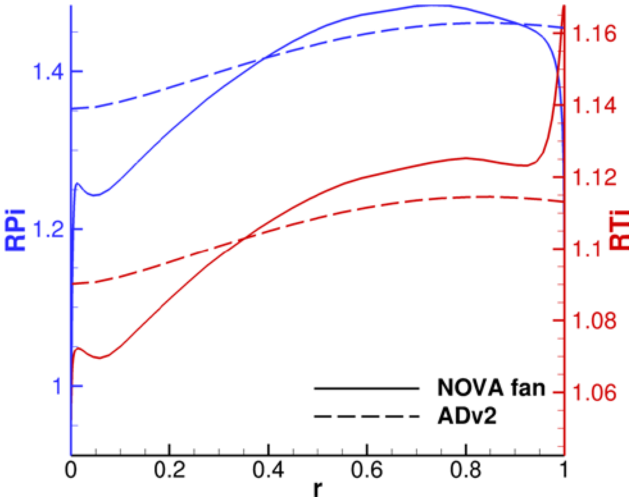

Figure 6 Radial distribution of stagnation pressure and temperature jumps for the NOVA fan/OGV and ADv2 at design point

CFD calculations were carried out with the elsA software using ADv1 and ADv2 for the NOVA "podded" and "BLI" configurations. A typical solution is shown in Figure 7.

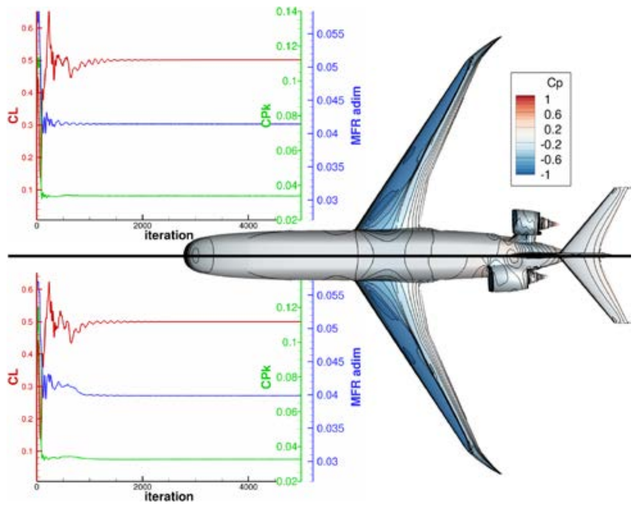

Figure 7 Typical elsA solution on the powered NOVA "podded" and "BLI" configurations

4.2 Aeropropulsive performance

A few quantities that will be used in the next figures have to be defined at this stage: R_X is the net stream-wise force coefficient (2) including the fan traction, CP_K the fan mechanical power coefficient (3), MFR_{adim} the mass flow coefficient (4) and C_t the fan traction coefficient (5).

$$R_X = \frac{F_X}{q_\infty S_{ref}} \quad (2)$$

$$CP_K = \frac{P_K}{q_\infty S_{ref} V_\infty} \quad (3)$$

$$MFR_{adim} = \frac{MFR}{\rho_\infty S_{ref} V_\infty} \quad (4)$$

$$C_t = \frac{T}{q_\infty S_{ref}} \quad (5)$$

In Figure 8, it can be observed that the BLI configuration mass flow is lower for the same Rx (a negative value of Rx means an excess of thrust). At "cruise" condition (Rx=0), the difference is about 5% with ADv1 and 4% with ADv2.

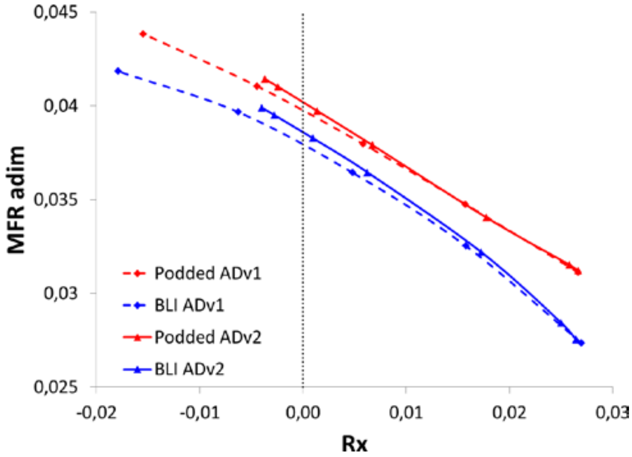

Figure 8 Mass flow rate coefficient versus net stream-wise force coefficient

The discrepancies between the two AD models are more important concerning the fan power prediction (see Figure 9), not only in absolute values but also between the podded and BLI configurations. Both AD models predict low to no BLI benefit at reduced fan power, which was expected given the aggressive shape of the engine inlet, leading to a massive separation at reduced mass flow. With higher thrust, a power advantage clearly appears using ADv2 while it is at best negligible using ADv1, or even negative. It is worth noting that higher thrust values could not be obtained using ADv2 not because of robustness issues, but because they corresponded to high rpm cases for which the in-house tool used to generate ADv2 input data reached a limit (non-realistic) supersonic speed at blade tip.

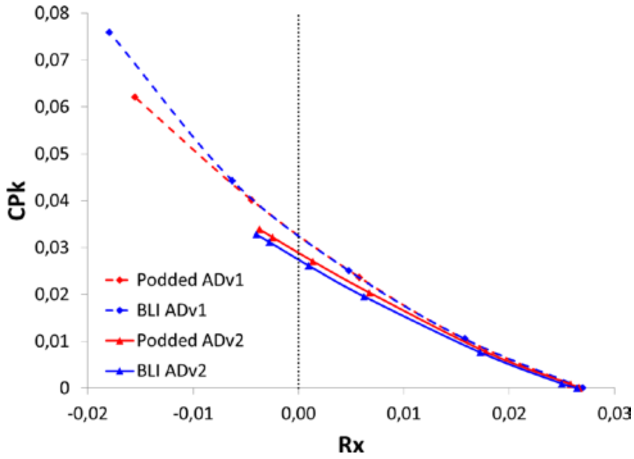

Figure 9 Fan power coefficient versus net stream-wise force coefficient

Another way to represent the BLI power advantage is to plot the PSC as in Figure 10. High (positive or negative) PSC values for Rx>0.02 correspond to very low power cases and are due to a low denominator value. While the PSC is mostly negative with ADv1, meaning that the podded configuration requires less power at same net force, it is positive with ADv2. At cruise condition (Rx=0), PSC=0,8% with ADv1 and PSC=5,2% with ADv2, this latter value being more in line with our initial estimation from §1.

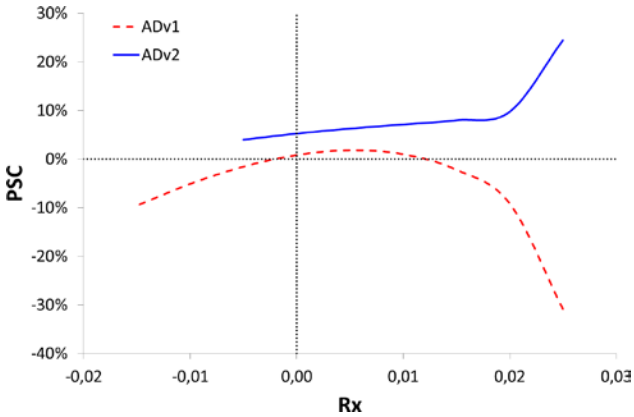

Figure 10 Power-saving coefficient versus net stream-wise force coefficient

To get a better understanding of the discrepancies between the two tested AD formulations, the analysis of the flow field in the vicinity of the disk can provide some insight. The next three figures are slices in the horizontal plane through the engine taken from cases with similar Rx (~-0.004).

The Mach number at fan face is quite different between the podded and BLI configurations, as illustrated in Figure 11. It also differs slightly depending on the AD formulation. With ADv1, it varies from 0.57 to 0.65 for the podded case, and from 0.15 to 0.79 for the BLI case. Whereas the distortion is more limited with ADv2, from 0.59 to 0.64 for the podded case, and from 0.2 to 0.7 for the BLI case.

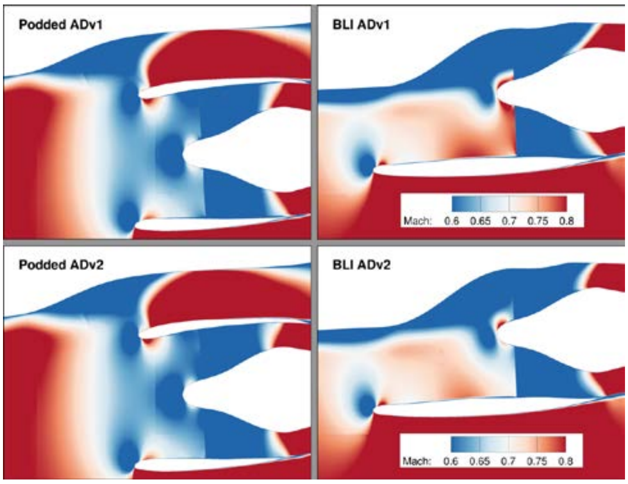

Figure 11 Mach number field in the podded and BLI inlets

The corresponding stagnation pressure and stagnation temperature jumps are displayed in Figure 12 and Figure 13 respectively. As expected, the results are highly dependent on the chosen AD formulation. Although both approaches lead to similar results in the podded case, the discrepancies are much higher in the BLI case. Assuming that a fan rotates at nominal rpm, the expected behavior depending on incoming flow Mach number would be the following:

- an increase of stagnation pressure jump and associated stagnation temperature jump for a Mach number lower than the design point Mach number;
- a decrease of stagnation pressure jump and associated stagnation temperature jump for a Mach number higher than the design point Mach number.

This corresponds to the behavior observed with ADv2, and this was expected since the local jumps are derived from interpolation in charts that include this fan physics. It is worth noticing in Figure 12 that when placed in the BLI configuration, the ADv2 tends to level the downstream stagnation pressure, since the jump is reduced in the region ingesting freestream air and increased in the BLI region.

Whereas the ADv1 formulation leads to a non-physical behavior and to a bias in fan power prediction, that cancels the mass flow advantage found in Figure 8, explaining the absence of substantial power saving with this fan model.

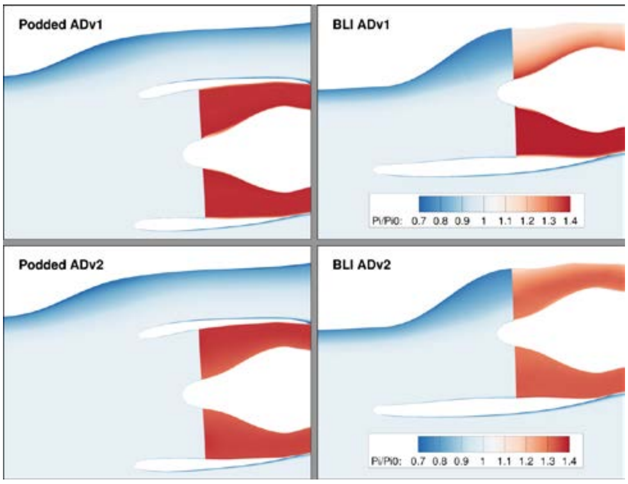

Figure 12 Effect of AD model on the stagnation pressure ratio for the "podded" and "BLI" configurations

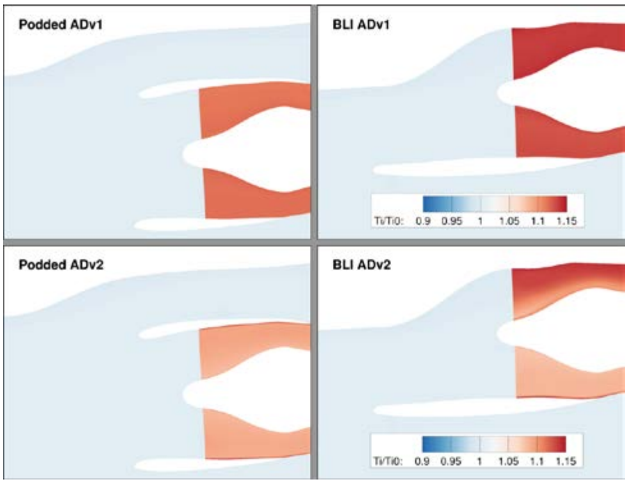

Figure 13 Effect of AD model on the stagnation temperature ratio for the "podded" and "BLI" configurations

5 Conclusion

From this study, the conclusion was drawn that the “helicopter” AD formulation is not suited for BLI benefit quantification. The “propeller” formulation better reproduces the underlying physics of a real fan, and in the NOVA case, it leads to a PSC value of about 5% at cruise conditions (M=0.82, CZ=0.5).

In order to further assess the capacity of such fan model to accurately predict traction and power values, results obtained with ADv2 on the podded configuration are compared to 3D RANS calculations for the NOVA fan/OGV in Figure 14 and Figure 15. The AD results stay within the NOVA fan/OGV operating domain, even if the absolute values of power at a given mass flow seem to be slightly underestimated by the AD. This could be explained either by the procedure used to generate the blade geometry and the associated interpolation charts at different rpm, or by more obvious differences between the two approaches, such as the absence of tip leakage flow in the AD case. However, this should not be a major obstacle for BLI power saving prediction.

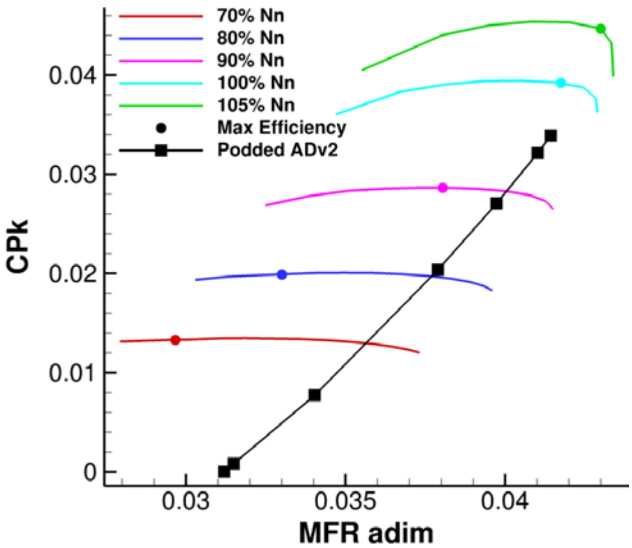

Figure 14 Fan power coefficient versus mass flow coefficient for the NOVA fan and the ADv2 model

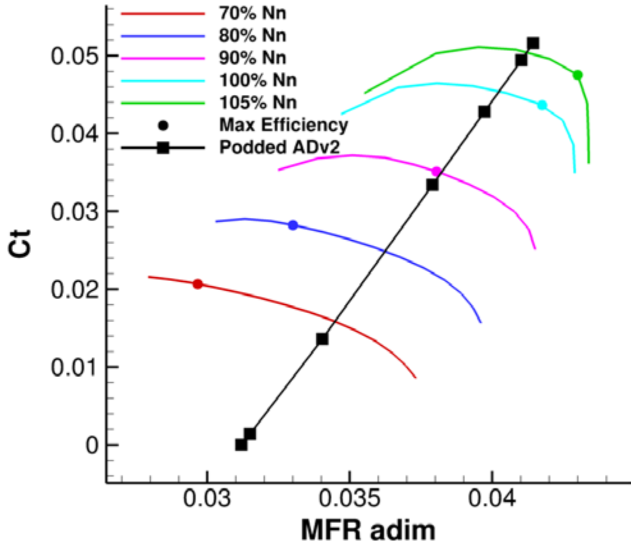

Figure 15 Fan traction coefficient versus mass flow coefficient for the NOVA fan and the ADv2 model

A more important object of concern is the capacity of such simplified fan model to reproduce efficiency loss due to off-design operation in a BLI case. Full annulus URANS calculation of the NOVA fan/OGV installed in the BLI configuration would provide some reliable data regarding that issue. An alternative to the URANS formulation would be to consider the "body-force" model, recently implemented in the elsA software. This affordable approach in a design phase can be considered as an intermediate step between the AD model and full annulus URANS computations. Indeed, advanced formulations of the body-force model aim at representing the overall fan performances (FPR, efficiency…), within a periodic time-averaged force field, including rotor-locked and rotating disturbances over a blade passage.

References

[1] Wiart L., Atinault O., Paluch B., Hue D. and Grenon R. Development of NOVA Aircraft Configurations for Large Engine Integration Studies, *33rd AIAA Applied Aerodynamics Conference*, June 22-26, 2015, Dallas, TX

[2] Smith L. H. Jr., Wake Ingestion Propulsion Benefit, *Journal of Propulsion and Power*, Vol. 9, No. 1, 1993, pp. 74–82

[3] Plas A., Performance of Boundary Layer Ingesting Propulsion System, MSc Thesis, Massachusetts Institute of Technology, 2006

[4] Uranga A., et al. Preliminary Experimental Assessment of the Boundary Layer Ingestion Benefit for the D8 Aircraft, *52nd Aerospace Sciences Meeting*, January 13-17, 2014, National Harbor, Maryland

[5] Cambier L., Heib S. and Plot S. The Onera elsA CFD Software: Input From Research and Feedback From Industry, *Mechanics & Industry* 14, (2013), 159-174.

[6] Colin Y., Deniau H. and Boussuge J.F. A Robust Low-Speed Preconditioning Formulation *Computers & Fluids*, 47 (2011), 1-15

[7] Moens F., Gardarein P. Numerical Simulation of the Propeller/Wing Interaction for transport aircraft *19th AIAA Applied Aerodynamics Conference* Anaheim, CA (USA), June 11-14, 2001

[8] Malard L., Bousquet J.-M., Atinault O., Larcher J.-L., Séchaud J.-F, High Speed Testing and CFD Investigations for the New Generation Military Transport Aircraft Development, *23rd AIAA Applied Aerodynamics Conference* Toronto, Canada, June 6-9 2005

[9] Atinault O., Carrier G., Grenon R., Verbeke C. and Viscat P. Numerical and Experimental Aerodynamic Investigations of Boundary Layer Ingestion for Improving Propulsion Efficiency of Future Air Transport, *31st AIAA Applied Aerodynamics Conference*, June 24-27, 2013, San Diego, CA

[10] Renaud T., Benoit C., Boniface J.-C., Gardarein P. Navier-Stokes Computations of a Complete Helicopter Configuration Accounting for Main and Tail Rotors Effects, *29th European Rotorcraft Forum*, Friedrichshafen, Germany, September 16-18, 2003

Contact Author Email Address

ludovic.wiart@onera.fr

Copyright Statement